FIRST PRINCIPLES STUDIES OF IONIC OXIDATION OF SULFUR DIOXIDE AND MOLECULAR CLUSTERING

NARCISSE TSONA

Division of Atmospheric Sciences

Department of Physics

Faculty of Science

University of Helsinki

Helsinki, Finland

Academic dissertation

To be presented, with the permission of the Faculty of Science of the University of Helsinki, for public criticism in auditorium E204, Gustaf Hällströmin katu 2, on June 3rd, 2016, at 12 o'clock noon.

Helsinki 2016

Author's Address: Department of Physics
                     P.O. Box 64
                     FI-00014 University of Helsinki
                     narcisse.tsonatchinda@helsinki.fi

Supervisors: Professor Hanna Vehkamäki, Ph.D.
                     Department of Physics
                     University of Helsinki

                     Doctor Nicolai Bork, Ph.D.
                     Infuser Denmark
                     University of Copenhagen

Reviewers: Professor Hannu Häkkinen, Ph.D.
                     Department of Physics
                     University of Jyväskylä

                     Doctor Mauritz Ryding, Ph.D.
                     Department of Chemistry
                     University of Oslo

Opponent: Professor Joel Thornton, Ph.D.
                     Department of Atmospheric Sciences
                     University of Washington

Acknowledgements

Narcisse Tchinda Tsona

University of Helsinki, 2016

Abstract

Sulfur oxidation products are involved in the formation of acid rain and atmospheric aerosol particles. The formation mechanism of these sulfur-containing species is often complex, especially when ions are involved. The work of this thesis uses computational methods to explore reactions of sulfur dioxide with some atmospheric ions, and to examine the effect of humidity on the stability and electrical mobilities of sulfuric acid-based clusters formed in the first steps of atmospheric particle formation.

Quantum chemical calculations are performed to provide insights into the mechanism of the reaction between sulfur dioxide (SO_2) and the superoxide ions (O_2^-) in the gas phase. This reaction was investigated in various experimental studies based on mass spectrometry, but discrepancies on the structure of the product remained disputed. The performed calculations indicate that the peroxy $SO_2O_2^-$ molecular complex is formed upon collision of SO_2 and O_2^-. Due to a high energy barrier, $SO_2O_2^-$ is unable to isomerize to the sulfate radical ion (SO_4^-), the most stable form of the singly charged tetraoxysulfurous ion. It is suggested that $SO_2O_2^-$ is the major product of SO_2 and O_2^- collision.

The gas-phase reaction between SO_2 and SO_4^- is further explored. From quantum chemical calculations and transition state theory, it is found that SO_2 and SO_4^- cluster effectively to form $SO_2SO_4^-$, which reacts fast at low relative humidity to form $SO_3SO_3^-$. This species has never been observed in the atmosphere and its decomposition upon collision with other atmospheric species is most likely. First-principles molecular dynamics simulations are used to probe the decomposition by collisions with ozone (O_3). The most frequent reactive collisions lead to the formation of SO_4^-, SO_3, and O_2. This implies that SO_4^- acts as a good catalyst in the SO_2 oxidation by O_3 to SO_3.

The best structures and the thermochemistry of the stepwise hydration of bisulfate ion, sulfuric acid, base (ammonia or dimethylamine) clusters are determined using quantum chemical calculations. The results indicate that ammonia-containing clusters are more hydrated than dimethylamine-containing ones. The effect of humidity on the mobilities of different clusters is further examined and it is finally found that the effect of humidity is negligible on the electrical mobilities of bisulfate ion, sulfuric acid, ammonia or dimethylamine clusters.

Keywords: sulfur dioxide, molecular clustering, kinetics, first principles methods

Contents

List of publications

This thesis consists of an introductory review, followed by four research articles. In the introductory part, these papers are cited according to their roman numerals. **Papers I** and **II** are reproduced with the permission of The Royal Society of Chemistry and the Creative Commons Attribution 3.0 License, respectively. **Papers III** and **IV** are reprinted with the permission of American Chemical Society.

I Tsona, T.N., Bork, N., and Vehkamäki, H. (2014). On the gas-phase reaction between SO_2 and $O_2^-(H_2O)_{0-3}$ clusters − an ab initio study, *Phys. Chem. Chem. Phys.*, 16:5987–5992.

II Tsona, T.N., Bork, N., and Vehkamäki, H. (2015). Exploring the chemical fate of the sulfate radical anion by reaction with sulfur dioxide in the gas phase, *Atmos. Chem. Phys.*, 15:495–503.

III Tsona, T.N., Bork, N., V. Loukonen, and Vehkamäki, H. (2016). A Closure Study of the Reaction between Sulfur Dioxide and the Sulfate Radical Ion from First−Principles Molecular Dynamics Simulations, *J. Phys. Chem. A*, 120:1046–1050.

IV Tsona, T.N., Henning, H., Bork, N., Loukonen, V., and Vehkamäki, H. (2015). Structures, Hydration, and Electrical Mobilities of Bisulfate Ion−Sulfuric Acid−Ammonia/Dimethylamine Clusters: A Computational Study, *J. Phys. Chem. A*, 119:9670–9679.

1 Sulfur oxidation products and their implication in atmospheric processes

Sulfur is important in many areas of human life. It possesses medicinal properties through some of its organic derivatives (Parcell, 2002; Omar and Al-Wabel, 2010) and participates in atmospheric processes through its oxidation products (Berndt et al., 2003, 2004; Seinfeld and Pandis, 2006; Shukla et al., 2013). Sulfur is predominatly present in the atmosphere as sulfur dioxide (SO_2), which is mainly emitted from volcanoes and human activities. The oxidation process of SO_2 is the main way by which sulfur is tranformed into other sulfur-containing compounds in the atmosphere. Atmospheric sulfur-containing compounds actively take part in acid rain and aerosol particle formation. Aerosol particles, very small liquid or solid particles suspended in air (Hinds, 1999), have various effects on human health (Stieb et al., 2002; Nel, 2005) and climate (Yu et al., 2001; Ramanathan et al., 2001). They are either emitted into the atmosphere as particles such as soot, pollen, or sea salt particle − known as primary aerosol particles−, or formed in the atmosphere from condensable vapours − known as secondary aerosol particles. Although believed to cool the climate, secondary aerosol particles constitute one of the major uncertainties in predicting the net radiative forcing and global temperature change (IPCC, 2013), although intensive research has been dedicated to aerosol science during the past decades.

It is well established that the formation of atmospheric aerosol particles in many environments is driven by sulfuric acid (H_2SO_4) (Kuang et al., 2008; Nieminen et al., 2009). Sulfuric acid forms very stable molecular clusters with ammonia, amines, and organic compounds (Kurtén et al., 2008; Almeida et al., 2013; Riccobono et al., 2014; Ehn et al., 2014). Other sulfur oxidation products than sulfuric acid are also known to enhance or trigger the formation of atmospheric aerosols (Berndt et al., 2008; Laaksonen et al., 2008; Bork et al., 2014; Chen et al., 2015). The main source of atmospheric H_2SO_4 is SO_2 oxidation reactions. These reactions can follow a completely electrically neutral mechanism, that is, without involving charged species, or they can be ion-induced. The electrically neutral oxidation of SO_2 in the gas phase, which includes reactions with the hydroxyl radical in a UV-light-induced mechanism (Seinfeld and Pandis, 2006), stabilized Criegee intermediates (Welz et al., 2012; Mauldin III et al., 2012), and mineral dust (Harris et al., 2013) is the major source of atmospheric H_2SO_4, while ion-induced oxidation constitutes a minor contribution (Enghoff et al., 2012; Bork et al., 2013a).

SO_2 reactions with ions are generally complex. Athough the terminal oxidation species is always H_2SO_4 or HSO_4^-, various oxysulfurous intermediate ions can form (Möhler et al., 1992; Fehsenfeld and Ferguson, 1974; Fahey et al., 1982). In cloud droplets, SO_2 oxidation leads to the formation of sulfates (Hegg et al., 1996).

Ions are produced in the atmosphere from galactic cosmics rays and from radon decay. The oxygen (O_2) and nitrogen (N_2) molecules are the most likely species to be ionized first, given their high concentration in the atmosphere. Due to its high electron affinity, O_2 most likely carries a negative charge, forming the superoxide ion (O_2^-), while N_2 carries a positive charge. Thereafter, a number of chemical reactions including charge transfer may take place. Various reactions of O_2^- with trace pollutants such as O_3, NO, NO_2, CO_2, and SO_2 have been investigated by experimental techniques (Fahey et al., 1982; Fehsenfeld and Ferguson, 1974; Möhler et al., 1992). Reactions with SO_2 are the most interesting in this context since sulfur oxidation products participate in the formation of atmospheric aerosol particles and contribute to the understanding of the atmospheric sulfur cycle. However, the use of experimental techniques such as mass spectrometry does not alone yield a clear understanding of the mechanism and species involved in chemical reactions. While giving information on the molecular weight of the species formed, from which their elemental composition can be obtained, mass spectrometry is not able to reveal the chemical formulae of the detected compounds. Also, some reactions happen so fast that they may not be captured. Furthermore, the formation mechanisms, identities and the chemical outcomes of some of these species remain poorly known. The work presented in this thesis aims to uncover detailed mechanisms of some SO_2 ion-induced oxidation reactions using quantum chemical and molecular dynamics simulations.

Recent advances in experimental methods to investigate atmospheric particle formation has led to the development of state-of-the-art instruments like the atmospheric pressure interface time-of-flight mass spectrometer (APi-ToF MS), which allows detection of molecular clusters down to 1 nm size (Junninen et al., 2010; Ehn et al., 2010). However, the ubiquitous water vapor, one of the most abundant trace gases in the atmosphere, is neither detected with most instruments including the APi-ToF MS nor taken into account in various dynamics simulations of atmospheric particle formation: the concentration of water is so high compared to that of sulfuric acid, ammonia or amines that the explicit kinetic and dynamic modelling of H_2SO_4-NH_3/amine-H_2O is

impossible (Olenius et al., 2013). Another challenge that comes with hydration is the separation of hydrated clusters using an ion mobility mass spectrometer. Water generally evaporates in the instrument and the clusters are detected in their dry states. Theoretical calculations demonstrated, nevertheless, that hydration might play a role on the dynamics of these clusters as water binds effectively to various sizes of electrically neutral H_2SO_4-based clusters (Henschel et al., 2014). Further calculations are performed in this thesis to investigate the hydration effect on electrical mobilities of H_2SO_4-based clusters.

The work presented in this thesis aims to:
− provide detailed mechanisms for reactions between SO_2 and some atmospheric ions, namely O_2^- and SO_4^-, in order to bridge the gap between theory and experiments (**Papers I & II**),
− investigate the effect of hydration on molecular clustering, reaction rate constants, and electrical mobilities of charged species (**Papers I, II & IV**),
− evaluate the steric effects on the reaction rate constants and the dynamics of clusters (**Paper III**).

2 Quantum chemical methods

The first step to treat physical and chemical problems using quantum chemistry is to solve the time-independent Schrödinger equation. This fundamental equation in quantum mechanics, which describes the stationary states of a system of electrons and atomic nuclei, is given as

$$\hat{H}\Psi(r, R) = E\Psi(r, R), \tag{1}$$

where E is the energy and $\Psi(r,R)$ the wavefunction describing the quantum state of the system. $\hat{H}$ is the Hamiltonian operator, which yieds the total energy (kinetic and potential) of the system when acting on the wavefunction. For a non-relativistic system containing N electrons and M nuclei, the Hamiltonian operator is given (in atomic units) as (Jensen, 2007)

$$\hat{H} = -\sum_{i=1}^{N} \frac{1}{2} \nabla_i^2 - \sum_{A=1}^{M} \frac{1}{2M_A} \nabla_A^2 - \sum_{1=1}^{N} \sum_{A=1}^{M} \frac{Z_A}{\hat{r}_{iA}} + \sum_{i=1}^{N} \sum_{j>1}^{N} \frac{1}{\hat{r}_{ij}} + \sum_{A=1}^{M} \sum_{B>1}^{M} \frac{Z_A Z_B}{\hat{R}_{AB}} \tag{2}$$

$$\equiv \hat{T}_e(r) + \hat{T}_N(R) + \hat{V}_{eN}(r, R) + \hat{V}_{ee}(r) + \hat{V}_{NN}(R). \tag{3}$$

$\hat{T}_e(r)$ and $\hat{T}_N(R)$ are the electron and nuclear kinetic energy operators, while $\hat{V}_{ee}(r)$, $\hat{V}_{eN}(r, R)$, and $\hat{V}_{NN}(R)$ decribes the electron-electron, electron-nuclear, and nuclear-nuclear interactions, respectively. $\hat{r}_{iA} = |\hat{r}_i - \hat{R}_A|$, $\hat{r}_{ij} = |\hat{r}_i - \hat{r}_j|$, and $\hat{R}_{AB} = |\hat{R}_A - \hat{R}_B|$ are distance operators between electron i and the nucleus A, between electrons i and j, and between the nuclei A and B, respectively. Solving the Schrödinger equation requires a set of assumptions and approximations, one of which is the Born-Oppenheimer (BO) approximation. This approximation assumes that the motion of atomic nuclei and the motion of electrons in a system can be separated. This is justified by the fact that the mass of an atomic nucleus in a molecule is much larger (more than 1000 times) than the mass of an electron. In dynamical sense, electrons move much faster than atomic nuclei, and can be assumed to be moving in a field of fixed nuclei. Indeed, electrons respond to forces very quickly while nuclei do not. The wavefunction describing the system can then be separated into nuclear wavefunction ($\chi_{nucl}(R)$) and electronic wavefunction ($\psi_{elec}(r, R)$) that depends on the (fixed) nuclear positions. On the other hand, the nuclear kinetic energy term in equation (3) can be neglected and we are left with the electronic part of the Halmiltonian

$$\hat{H}_{elec}(r, R) = \hat{T}_e(r) + \hat{V}_{eN}(r, R) + \hat{V}_{ee}(r) + \hat{V}_{NN}(R). \tag{4}$$

We can then write the electronic Schrödinger equation as

$$\hat{H}_{\text{elec}}(r, R)\psi_{\text{elec}}(r, R) = E_{\text{elec}}(R)\psi_{\text{elec}}(r, R), \tag{5}$$

where $\psi_{\text{elec}}(r, R)$ and the electronic energy $E_{\text{elec}}(R)$ are solutions to Equation (5). It should be noted here that although the nuclear kinetic energy term is solved separately under the BO approximation, this approximation still takes into account the positions of the nuclei upon which the electronic energy parametrically depends. The nuclear-nuclear interaction potential $\hat{V}_{\text{NN}}(R)$ is also often separated from equation (4) since the nuclear positions are parameters so that $\hat{V}_{\text{NN}}(R)$ is just a constant that shifts the eigenvalue by some fixed amount. The combination of $E_{\text{elec}}(R)$ with $\hat{V}_{\text{NN}}(R)$ forms the potential energy function which controls the nuclear motion. The nuclear Schrödinger equation can then be written as

$$\left(\hat{T}_{\text{N}}(R) + E_{\text{elec}}(R) + \hat{V}_{\text{NN}}(R)\right)\chi_{\text{nucl}}(R) = E\chi_{\text{nucl}}(R). \tag{6}$$

The total energy (E) of the system is obtained by solving equation (6). To any nuclear position corresponds an energy for the system but, in the calculations performed in this thesis, we are interested in the ground state global minimum geometry, that is, the best possible arrangement of the electrons and the nuclei of the system. Two main groups of methods are used in quantum chemistry to determine the ground state energy a system: wavefunction-based methods and density functional theory.

2.1   Wavefunction-based methods

To simplify the dynamics of a N-electron system in wavefunction-based quantum chemical methods, electron-electron interactions are approximated to interactions between one electron and the average field generated by the other electrons of the system. This is the so-called Hartree-Fock (HF) theory. Under this theory, the total electronic wavefunction is given as the product of the one-electron wavefunctions, $\phi(\vec{r}_{\text{i}})$, also known as spin orbitals, since they must contain both the spatial and spin components. The combination of the spin orbitals must obey the Pauli exclusion principle requirement so that the product wavefunction is antisymmetric with respect to interchanging any two electrons. This combination with the requirements therein can be achieved by writing

the product wavefunction in the form of a Slater determinant as

$$\Phi^{\mathrm{SD}} = \frac{1}{N!} \begin{vmatrix} \phi_1(\vec{r}_1) & \phi_2(\vec{r}_1) & \cdots & \phi_{\mathrm{N}}(\vec{r}_1) \\ \phi_1(\vec{r}_2) & \phi_2(\vec{r}_2) & \cdots & \phi_{\mathrm{N}}(\vec{r}_2) \\ \cdots & \cdots & \ddots & \cdots \\ \phi_1(\vec{r}_{\mathrm{N}}) & \phi_2(\vec{r}_{\mathrm{N}}) & \cdots & \phi_{\mathrm{N}}(\vec{r}_{\mathrm{N}}) \end{vmatrix}. \tag{7}$$

In order to approximately solve the electronic Schrödinger equation under the HF theory, one makes the assumption that the product wavefunction of a N-electron system can be approximated by a single Slater determinant made up of one spin orbital per electron. The HF method determines the set of spin orbitals which minimize the energy of the system and give the best possible single Slater determinant. This is done by applying the *variational principle* and as a result, we obtain a set of N HF equations defining the orbitals,

$$\left(\frac{1}{2} \nabla_{\mathrm{i}}^2 - \sum_{A=1}^{M} \frac{Z_{\mathrm{A}}}{|\vec{r}_1 - \vec{R}_{\mathrm{A}}|} \right) \phi_{\mathrm{i}}(\vec{r}_1) + \sum_{j \neq i} \left(\int \phi_{\mathrm{j}}^*(\vec{r}_2) \frac{1}{|\vec{r}_1 - \vec{r}_2|} \phi_{\mathrm{j}}(\vec{r}_2) \, d\vec{r}_2 \right) \phi_{\mathrm{i}}(\vec{r}_1)$$

$$- \sum_{j \neq i} \left(\int \phi_{\mathrm{j}}^*(\vec{r}_2) \frac{1}{|\vec{r}_1 - \vec{r}_2|} \phi_{\mathrm{i}}(\vec{r}_2) \, d\vec{r}_2 \right) \phi_{\mathrm{j}}(\vec{r}_1) = \varepsilon_{\mathrm{i}} \phi_{\mathrm{i}}(\vec{r}_1), \quad (8)$$

where ε_{i} is the energy eigenvalue associated with the spin orbital ϕ_{i}. The solution of HF equations for a given spin orbital depends on the solution of other orbitals. To solve the HF equations, one needs to guess some initial orbitals and then refine the guesses iteratively. This process is called the *self-consistent-field* (SCF) approach. The terms from left to right on the left hand side of equation (8) are kinetic energy, electron-nuclear coulombic attraction, electron-electron coulombic repulsion also known as the *Coulomb term*, and electron-electron exchange interactions also known as *exchange term*. The exchange term arises from the antisymmetry of the wavefunction as required by the Pauli exclusion principle. Taking the expectation value of the electronic Hamiltonian (equation (4)) using the Slater determinant (equation (7)),$\langle \Phi^{\mathrm{SD}} | \hat{H}_{\mathrm{elec}}(r, R) | \Phi^{\mathrm{SD}} \rangle$, yields

the HF energy

$$E^{\mathrm{HF}} = \sum_{i=1}^{N} \int \phi_{\mathrm{i}}^{*}(\vec{r}_1) \left(-\frac{1}{2} \bigtriangledown_{\mathrm{i}}^{2} + v_{\mathrm{ext}}(r) \right) \phi_{\mathrm{i}}(\vec{r}_1) \ d\vec{r}_1$$

$$+ \sum_{i=1}^{N} \sum_{j}^{N} \int \int \phi_{\mathrm{i}}^{*}(\vec{r}_1) \phi_{\mathrm{j}}^{*}(\vec{r}_2) \frac{1}{|\vec{r}_1 - \vec{r}_2|} \phi_{\mathrm{i}}(\vec{r}_1) \phi_{\mathrm{j}}(\vec{r}_2) \ d\vec{r}_1 d\vec{r}_2$$

$$+ \sum_{i=1}^{N} \sum_{j}^{N} \int \int \phi_{\mathrm{i}}^{*}(\vec{r}_1) \phi_{\mathrm{j}}^{*}(\vec{r}_2) \frac{1}{|\vec{r}_1 - \vec{r}_2|} \phi_{\mathrm{j}}(\vec{r}_1) \phi_{\mathrm{i}}(\vec{r}_2) \ d\vec{r}_1 d\vec{r}_2. \quad (9)$$

According to the variational principle, this energy is an upper limit to the expectation value obtained using the true ground state wavefunction (*i.e.,* the ground state energy).

The difference between the true ground state energy and the HF energy for a given set of spin orbitals is known as the *correlation energy*. This difference in energy is due to the fact that the influence of electrons coming close to each other at some point is not taken into account in the description of electron interactions within the HF wavefunction. Although the correlation energy accounts only for a small fraction of the total energy, it is usually very important for chemical purposes. The correlation energy can be calculated with more sophisticated methods often called *post Hartree-Fock methods*, of which the most widely used are the configuration interaction (CI), the Møller Plesset (MP) perturbation theory, and the coupled cluster (CC) theory. The CI method constructs the wavefunction as a linear combination of Slater determinants, with the expansion coefficients determined using the variational principle. This method allows the ground state wavefunctions of a system to mix with it excited state wavefunctions. The level of excitations, single, double, triple, etc., gives rise to CIS, CISD, CISDT methods, respectively. A full CI implies all possible excitations of the Slater determinants and thus corresponds to exactly solving the Schrödinger equation. The CI calculations require large computational ressources and this method is generally limited to relatively small systems. The MP perturbation theory (Møller and Plesset, 1934) calculates the correlation energy by adding a small perturbation to an unperturbed Hamiltonian operator and solving the *perturbed* Schrödinger equation. First, second, third, fourth, etc., orders perturbation leads to MP1, MP2, MP3, MP4 methods, repectively. The first actual improvement over the HF energy with these methods is at the MP2 level. MP2 is the most affordable method including electron correlation and it can account for $80-90$ % of the correlation energy (Jensen, 2007). CI and MP are not used in any calculations in this thesis.

Coupled cluster methods use an exponential expansion of the wavefunction to account for electron correlation. In the CC theory, the exact wavefunction is written as (Jensen, 2007)

$$\Psi = e^{\hat{T}}\Phi_0 \tag{10}$$

$$= \left(1 + \hat{T} + \frac{1}{2}\hat{T}^2 + \frac{1}{3!}\hat{T}^3 + \cdots + \frac{1}{N!}\hat{T}^N\right)\Phi_0, \tag{11}$$

where Φ_0 is the single determinant wavefunction, usually the HF determinant, and the cluster operator $\hat{T}$ the sum of operators $\hat{T}_1, \hat{T}_2, \hat{T}_3, \cdots, \hat{T}_N$, that generate singly-excited, doubly-excited, triply-excited, $\cdots$, Nth excited Slater determinants. N is the number of electrons of the system. All possible excited determinants are generated when all operators are included in the cluster operator $\hat{T}$, and this is equivalent to the full CI, which is unfeasible for big systems. The expansion of $\hat{T}$ is truncated and the accuracy of the method depends on the level of truncation. The lowest truncation giving rise to a significant improvement over HF for the ground state energy is CCSD, which refers to coupled cluster with single and double excitations (here $\hat{T} = \hat{T}_1 + \hat{T}_2$). Alternatively, there is CCSDT (when $\hat{T} = \hat{T}_1 + \hat{T}_2 + \hat{T}_3$), CCSDTQ (when $\hat{T} = \hat{T}_1 + \hat{T}_2 + \hat{T}_3 + \hat{T}_4$), etc. The most commonly used coupled cluster method is the CCSD(T) (used in **papers I** and **II**), which includes "*normal*" single and double excitations, but a perturbative extimate of the triple excitations (Purvis and Bartlett, 1982). Other variants of the coupled cluster (used in **paper IV**) are the CC2 method (Christiansen et al., 1995) and the RI-CC2 (Hättig and Weigend, 2000), derived from CCSD and where the doubles excitations arise from MP2.

2.2   Density functional theory

The high computational cost is a challenge and often a limitation for treating systems with a large number of electrons using wavefunction-based methods. Density functional theory (DFT) is a partial solution to this problem. Instead of the many-body wavefunction used in HF theory, Hohenberg and Kohn (Hohenberg and Kohn, 1964) proved that for N interacting electrons moving in an external potential $V_{\text{ext}}(\vec{r})$, the ground state electron density, ρ, uniquely determines the exact ground state electronic energy. While the wavefunction for an N electron system contains $4N$ variables (three spartial and one spin coordinate) for each electron, the electron density depends on three spatial coordinates independently of the system size. The central quantity in

DFT is the electron density, defined as the square of the wavefunction of the system integrated over all but one of the spatial variables,

$$\rho(\vec{r}) = N \int \cdots \int |\Psi(\vec{r}_1, \vec{r}_2, \cdots, \vec{r}_N)|^2 \ d\vec{r}_2 \cdots d\vec{r}_N, \tag{12}$$

where $\rho(\vec{r})$ determines the probability of finding any of the N electrons within the volume element $d\vec{r}$. The electron density is a non-negative function which vanishes at infinity $(\rho(\vec{r} \to \infty) = 0)$ and integrates to the number of electrons in the system $\left(\int \rho(\vec{r})d\vec{r} = N\right)$. According to the first Hohenberg-Kohn theorem, the total ground state energy of a many-electron system is a functional of the electron density. This means that if we know the electron density functional, we know the total energy of the system. Now, the major problem in DFT arises: the exact functional is generally not known.

Although the Hohenberg-Kohn theorem was established as the basis of modern DFT, the significant breakthrough of this method was achieved in 1965 when Kohn and Sham developed a variational approach that uses an independent-electron approximation of kinetic energy, similarly to the HF method (Kohn and Sham, 1965). They suggested to calculate the kinetic energy assuming non-interacting electrons

$$T_s = -\frac{1}{2} \sum_{i=1}^{N} \int \phi_i^*(\vec{r}) \bigtriangledown^2 \phi_i(\vec{r}) \ d\vec{r}, \tag{13}$$

which is only an approximation of the exact kinetic energy. Just as the HF method, this approximation provides about 99 % of the exact kinetic energy. Here the electron density is approximated in terms of one-electron orbitals similarly to the Slater determinant

$$\rho(\vec{r}) = \sum_{i=1}^{N} |\phi_i(\vec{r})|^2. \tag{14}$$

The difference between the exact kinetic energy and that calculated with the independent-electron approximation is accounted for in the so-called *exchange-correlation* term, E_{XC}. Under the Kohn-Sham theory, the functional energy can then be expressed as a sum of four terms below,

$$E[\rho(\vec{r})] = T_s[\rho(\vec{r})] + E_{ne}[\rho(\vec{r})] + J[\rho(\vec{r})] + E_{XC}[\rho(\vec{r})], \tag{15}$$

where E_{ne} is the coulombic attraction between the nuclei and electrons

$$E_{ne}[\rho(\vec{r})] = \int V_{ext}(\vec{r})\rho(\vec{r}) \ d\vec{r}, \tag{16}$$

J is the coulombic repulsion between the electrons

$$J[\rho(\vec{r})] = \frac{1}{2} \int \int \frac{\rho(\vec{r})\rho(\vec{r'})}{\vec{r} - \vec{r'}} \, d\vec{r} d\vec{r'}. \tag{17}$$

E_{XC} represents the kinetic correlation energy and the potential correlation and exchange energy. The two difficult terms to calculcate in equation (15) are $T_{\mathrm{s}}[\rho(\vec{r})]$ and $E_{\mathrm{XC}}[\rho(\vec{r})]$. While $T_{s}[\rho(\vec{r})]$ can be readily determined if the set of orbitals $\phi_{\mathrm{i}}(\vec{r})$ is known, $E_{\mathrm{XC}}[\rho(\vec{r})]$ can be determined from different methods using various approximations. From the second Hohenberg-Kohn theorem (Hohenberg and Kohn, 1964) the functions $\phi_{\mathrm{i}}(\vec{r})$ that minimize the energy can be determined, analogously to the variational principle, by solving the set of N Kohn-Sham equations

$$\left(-\frac{1}{2} \nabla^2 + \int \frac{\rho(\vec{r})\rho(\vec{r'})}{\vec{r} - \vec{r'}} \, d\vec{r'} + V_{\mathrm{ext}}(\vec{r}) + V_{\mathrm{XC}}(\vec{r}) \right) \phi_{\mathrm{i}}(\vec{r}) = \phi_{\mathrm{i}}(\vec{r})\epsilon_{\mathrm{i}}(\vec{r}), \tag{18}$$

where $V_{\mathrm{XC}}(\vec{r})$ is the exchange-correlation potential defined as

$$V_{\mathrm{XC}}(\vec{r}) = \frac{\partial E_{\mathrm{XC}}[\rho(\vec{r})]}{\partial \rho(\vec{r})}. \tag{19}$$

The Kohn-Sham equations are similar to HF equations in the sense that they are derived in analogous ways and are both solved iteratively. However, the main difference in the two methods is that their exchange-correlation terms have different meaning (Koch and Holthausen, 2000). Furthermore, the Kohn-Sham theory would give the exact energy if the exact forms of E_{XC} and V_{XC} were known, whereas the HF theory is always an approximation.

The local density approximation (LDA) is the simplest formulation and it is the basis of all approximations of exchange-correlation functionals. In the LDA, the functional is approximated by the exchange-correlation functional of a uniform electron gas. LDA generally gives very good results for systems whose charge densities vary slowly. The most accurate results for the LDA exchange-correlation functional were obtained from Quantum Monte Carlo calculations by Ceperley and Alder (Ceperley and Alder, 1980). Since LDA is primarily designed for homogeneous systems, its limitations lie in overbinding of molecules, weakly bonded systems and solids. LDA is therefore not suitable for studying systems investigated in this thesis.

The first improvement of the LDA by including gradient corrections to the density

leads to the generalized gradient approximations (GGA). GGA uses not only the information about the density at the point where the functional is calculated, but also on its derivatives, in order to account for the non-homogeneity of the electron density. Amongst the most widely used GGA functionals are the PW91 (Perdew et al., 1992, 1996a) and PBE (Perdew et al., 1996b), used in **papers II** and **III** of this thesis. Furthermore, the D3 dispersion correction (Grimme et al., 2010) was used with the PBE functional in **paper III** to account for dispersion forces.

The natural development after the GGA leads to meta-GGA functionals and hybrid or hyper-GGA functionals. The meta-GGA functionals include the second derivative of the electron density, while the hybrid-GGA functionals mix a component of the exact HF exchange integral with the GGA component. One of the most commonly used versions of the hybrid-GGA is B3LYP (Becke, 1993). B3LYP was used in **papers II** and **IV**. A long-range corrected version of B3LYP, CAM-B3LYP (Yanai et al., 2004), which is a modification of B3LYP by including increasing HF exchange at increasing distances, was used in **papers I** and **II**. The B3LYP functional includes a constant amount of 20 % HF exchange (and hence 80 % B88 echange), whereas the amount of HF exchange varies from 19 to 85 % in the CAM-B3LYP functional depending on the distance. In particular, the increased amount of exact HF exchange has been shown to be advantageous when treating anions since the associated diffuse orbitals are ill described by pure B88 exchange functional (Yanai et al., 2004).

2.3   Basis sets

Having decided on the method (either wavefunction-based or DFT) to use in electronic structure calculations, another important part of the calculations is to build suitable sets of functions used to create the molecular orbitals, the *basis sets*. Typically, each of these functions is an one-electron spin orbital, similar to the functions $\phi_i(\vec{r})$ in HF and Kohn-Sham equations (equations (8) and (18), respectively). Each function $\phi_i(\vec{r})$ is expanded as a linear combination of some L known basis functions $f_k(\vec{r})$

$$\phi_i(\vec{r}) = \sum_{k=1}^{L} C_{ki} f_k(\vec{r}), \tag{20}$$

with coefficients C_{ki} to be determined.

Two types of basis functions are commonly used in the literature: *Slater type orbitals* (Slater, 1930) and *Gaussian type orbitals* (Boys, 1950). These are atom-centered orbitals, where the electron position is at a distance r from the atomic nucleus. Although the Slater type orbitals, with an e^{-r} dependence, accurately describe the behavior of electrons and have a rapid convergence with increasing number of functions, they are computationally challenging. Gaussian type orbitals have an e^{-r^2} dependence and, in this regard, fail to represent the behavior of the electron both near and far from the nucleus. However, they are computationally more affordable than the Slater type orbitals (Szabo and Ostlund, 1996). For the sake of accurate yet computationally affordable calculations, Slater type orbitals can be approximated as linear combinations of Gaussian type orbitals. Generally, three times as many Gaussian type orbitals as Slater type orbitals are needed to achieve similar accuracy.

Besides the choice of the type of basis functions, it is important to determine the number of these functions that are included in the basis set. The smallest number of basis functions required to contain all electrons of a system defines the so-called *minimum basis set*. Increasing the number of basis functions in the basis sets is a form of improvement which leads to a more flexible description of the electronic structure, however increasing the computational cost. The first improvement, which consists of doubling the number of basis functions in the minimum basis, produces a *Double Zeta* (generally denoted as DZ) type basis set. Chemical bonding generally involves exclusively the valence orbitals and hence, doubling or tripling the number of basis functions affects the valence orbitals only and we can talk of *Valence Double Zeta* (VDZ) basis set, for example, when the number of basis functions in the minimum basis set is doubled. Alternatively, there are *Valence Triple/Quadruple/Quintuple/Sextuple Zeta (VTZ, VQZ, V5Z, V6Z)* basis sets. Additional flexibility of the basis sets can be achieved by adding polarization functions or multiple sets of polarization functions, which are generally denoted in the basis sets by "p" or "P". The polarization within a basis set allows the molecular orbitals to be more asymetric about the nucleus. Another form of improvement of the basis set is to add diffuse functions, symbolized by "aug", "$+$", or "D". These functions accurately describe the wavefunction far from the nucleus and are highly important in describing systems with loosely bound species such as anions. For calculations involving electron

correlations, the use of *Dunning basis sets* (Dunning, 1989) is useful to achieve systematic covergence to the complete basis set limit. These basis sets are indicated by "*cc-p*", which stands for *correlation-consistent polarized*. One can have, for example, "*aug-cc-pVDZ*", standing for correlation-consisted valence double zeta basis set with diffuse functions.

2.4 Thermochemistry

Electronic structure calculations mainly aim at determining ground state energies at the temperature $T = 0$ K. However the free energies at non-zero temperatures are the important quantities used to understand or explain the chemistry of a system. The free energies are obtained by considering the contributions of translational, vibrational and rotational degrees of freedom in addition to the ground state electronic energies. This is done by means of statistical mechanics from the total partition function, q_{tot}, of the system under some assumptions. It is first assumed that the different contributions are separated from each other so that the total partition function can be written as $q_{tot} = q_{elec} q_{trans} q_{vib} q_{rot}$. The enthalpy ($H_i$) and entropy ($S_i$) are calculated from each partition function q_i as (McQuarrie, 1973)

$$H_i = k_B T^2 \left(\frac{\partial \ln q_i}{\partial T} \right)_V + k_B T V \left(\frac{\partial \ln q_i}{\partial V} \right)_T, \tag{21}$$

$$S_i = k_B T \left(\frac{\partial \ln q_i}{\partial T} \right)_V + k_B \ln q_i, \tag{22}$$

where T is the temperature, V the volume, and k_B the Boltzmann constant. The total enthalpy and entropy are determined by taking the sum of all the contributions, $H_{tot} = \sum H_i$ and $S_{tot} = \sum S_i$, respectively, wherefrom the Gibbs free energy is calculated:

$$G_{tot} = H_{tot} - T S_{tot}. \tag{23}$$

To calculate the electronic partition function, only the ground state electronic energy (E_0) is considered and it is assumed to be non-degenerate

$$q_{elec} = e^{-E_0/k_B T}. \tag{24}$$

The translational partition function is calculated by assuming ideal gas behavior and it is given as

$$q_{trans} = \left(\frac{2\pi M k_B T}{h^2} \right)^{3/2} \frac{k_B T}{P}, \tag{25}$$

where M is the mass and P the partial pressure of the molecule or cluster, often taken to be the standard pressure, 1 atm. h is the Planck constant.

The vibrational partition function is mostly calculated by assuming all vibrations to be harmonic and by considering only the real vibrational modes (*i.e.,* modes with

no negative frequencies), each mode having a *characteristic vibrational temperature* $\Theta_{\mathrm{vib,K}} = h\nu_{\mathrm{K}}/k_{\mathrm{B}}$, where ν is the frequency of the vibrational mode K.

$$q_{\mathrm{vib}} = \prod_{K}^{N_{\mathrm{vib}}} \frac{e^{-\Theta_{\mathrm{vib,K}}/2T}}{1 - e^{-\Theta_{\mathrm{vib,K}}/T}}, \tag{26}$$

N_{vib} is the total number of vibrational modes. It is equal to $(6 \times (\text{number of atoms}) - 6)$ for clusters and non-linear molecules, and $(6 \times (\text{number of atoms}) - 5)$ for linear molecules. Equation (26) gives the contribution to the vibrational energy at a temperature T different from zero. However, even at absolute 0 K temperature, the molecule or cluster retains a vibrational energy called *zero-point vibrational energy*, (*ZPVE*). This energy is given as $1/2 \sum_{K} h\nu_{\mathrm{K}}$.

The final assumption made to calculate the partition function is to treat the molecule or cluster as rigid rotor when determining the rotational contributions. Different forms of the rotational partition functions exist, depending on the symmetry of the system. For single atoms, $q_{\mathrm{rot}} = 1$. This case is not treated in this thesis. For systems investigated in this thesis, the rotational partition function is

$$q_{\mathrm{rot}} = \begin{cases} \dfrac{1}{\sigma} \left(\dfrac{8\pi^2 k_{\mathrm{B}} T}{h^2} \right) I & \text{for linear molecules} \\[3ex] \dfrac{\pi^{1/2}}{\sigma} \left(\dfrac{8\pi^2 k_{\mathrm{B}} T}{h^2} \right)^{3/2} (I_{\mathrm{x}} I_{\mathrm{y}} I_{\mathrm{z}})^{1/2} & \text{for non-linear polyatomic molecules and clusters,} \end{cases} \tag{27}$$

where σ is the rotational symmetry number, *i.e.,* the number of rotations bringing the molecule or cluster to identical configurations, I and I_{i} are the moments of inertia around the principal axes.

Although the approximations made in calculating the partition function make the calculations computationally affordable, they might lead to errors in the free energies (Kathmann et al., 2007; Loukonen et al., 2014). Specifically, the harmonic approximation is not valid in the case of hydrogen bonded molecular clusters and is often the worst approximation in determining the thermal contributions to the energies. However, there is no exact way of including anharmonic effects in the vibrational contributions although several approaches have been developed to solve the inharmonicity. These approaches, aimed at determining anharmonic scaling factors for harmonic frequencies, generally work for very small systems (Chaban et al., 1999; Barone, 2004; Scott and Radom, 1996). Since these scaling factors are derived from specific systems,

they depend on inter- and intramolecular vibrations, and may therefore be erroneous when applied to other systems (Loukonen et al., 2010). No scaling factors were used in this thesis.

All quantum chemical calculations of the thermal contributions and the free energies (equation (23)) were performed using DFT methods with the Gaussian 09 package (Frisch et al., 2009). It is known that the most important contribution to the free energies, the ground state electronic energy, is not accurately determined by DFT due the poor evaluation of electron correlation effects. Instead, post Hartree-Fock methods, which determine the correlation energies in a more accurate way than both HF and DFT, were used to calculate the ground state electronic energies (E_{elec}). The Gibbs free energies of molecules and clusters in **Papers I, II and IV** were therefore calculated as

$$G = E_{\mathrm{elec}} + G_{\mathrm{therm}} \tag{28}$$

where E_{elec} is calculated with the CCSD(T) method (**Paper I & II**) using Molpro (Werner et al., 2012) and with the RI-CC2 method (**Paper IV**) using the TURBO-MOLE program (Ahlrichs et al., 1989). G_{therm} is the zero-point corrected thermal energy, calculated with DFT. For a system where multiple configurations, including the most stable configuration, coexist within a certain energy range (*e.g.*, 3 kcal/mol as was chosen in **Paper IV**), a term accounting for the contributions due to multiple configurations is added to G (Ho et al., 2015):

$$G_{\mathrm{conf}} = -RT \ln \sum_{j} \exp\left(-\frac{G_j}{RT}\right). \tag{29}$$

In equation (29), R is the molar gas constant, T is the absolute temperature, and G_{j} is the Gibbs free energy of the configuration j relative to the most stable configuration.

3 First-principles molecular dynamics

Molecular dynamics (MD) methods are an efficient approach to simulate the movement of particles (atoms or molecules) in a given environment by integrating Newton's equation of motion,

$$\vec{F}_{\text{i}}(t) = M_{\text{i}}\frac{d^2\vec{R}_{\text{i}}(t)}{dt^2},$$
(30)

where $\vec{F}_{\text{i}}(t)$ is the force acting on the particle i having the mass M_{i}, and $\vec{R}_{\text{i}}$ is the position of the particle at time t. For a system of interacting particles, the phase-space trajectory is determined by solving equation (30). The forces between particles are calculated using either classical force fields or quantum mechanics. The success of MD relies strongly on how these forces are calculated, *i.e.,* how interactions between the particles are described. Classical force fields use predefined potentials that are developed to yield satisfactory results to specific systems. However, changing a single species in the system implies the parametrization of new potentials. In the context of the work of this thesis, where there is change in chemical bonding pattern, classical force fields would typically provoke an extra amount of efforts to develop new potentials adapted to new chemical products.

First-principles molecular dynamics (FPMD) is an alternative technique that calculates the interactions of particles and the resulting forces using quantum mechanics. FPMD has the advantage over the classical force fields MD of being suitable to study chemical reactions where the electronic structure changes during the dynamics, such as systems involving breaking or formation of bonds. Of the different approaches in FPMD, we used the Born-Oppenheimer MD approach which assumes decoupled motions of electrons and nuclei, similarly to the approximation made in solving the Schrödinger equation in Section 2. In these simulations, the dynamics of the atomic nuclei are treated classically, while the interaction forces are determined from the electronic structure calculations by taking the derivative of the energy with respect to the nuclear coordinates, $\vec{R}_{\text{i}}(t)$ (Marx and Hutter, 2009). This approach was used in **Paper III**, and the electronic structure was solved using DFT. A practical algorithm for the BO-FPMD can be summarized as follows:

- set initial nuclear positions and velocities, $\vec{R}_{\text{i}}(t)$ and $\vec{V}_{\text{i}}(t)$, respectively,

- evaluate the ground state energy, $\vec{E}_i(\vec{R}, t)$, and take its derivative with respect to $\vec{R}_i$ to obtain the forces acting on the nuclei,

- integrate the Newton's equation of motion to obtain new positions, $\vec{R}_i(t + \Delta t)$, and velocities, $\vec{V}_i(t + \Delta t)$,

- solve the electronic structure at the new nuclear positions $\vec{R}_i(t + \Delta t)$, calculate the forces arising from the new energy,

- integrate the system for other Δt, as needed.

The timestep, Δt, is the time interval between consecutive updates. In general, too long timesteps may lead to unrealistic behavior of the nuclear motion while too short timesteps make the simulation too slow. For smooth dynamics, a timestep of ~ 10 times lower than the highest vibrational frequency is recommended (Marx and Hutter, 2009). In **Paper III**, a timestep of 0.5 fs was used and the simulations were run for at least 600 fs, the minimum time at which a decisive outcome of the collision could be obtained. All simulations were performed using the Quickstep module (VandeVondele et al., 2005) of the CP2K package (www.cp2k.org). Special care was taken in selecting the initial velocities of the atoms in the system. These were obtained from short simulations with constant number of particles, constant volume and constant temperature, and from Maxwell-Boltzmann distribution of speeds (Atkins and de Paula, 2006). A suitable simulation cell size should lead to the convergence of both the energy and the dipole moment (Bork et al., 2013b). We used a cell size of $30 \times 30 \times 30$ Å ^{3} in all simulations in **Paper III**. The atomic coordinates at the begining of the simulations were taken from structures initially optimized using DFT (**Paper II**), which we re-optimized using CP2K.

Molecular dynamics simulations are usually performed in different ensembles, depending on the phenomena and the system properties investigated. In this thesis, the *microcanonical ensemble* labelled *NVE*, and the *canonical ensemble* labelled *NVT* were used. The *NVE* ensemble operates at constant number of particles, volume and total energy, therefore describing the dynamics of an isolated system. Assuming no other external forces than the forces between the particles of the system, the trajectory of the system in phase space is confined to the constant energy surface. The total energy is the sum of the potential energy, which is the electronic ground state energy, and the kinetic energy, which may be calculated at any time from particle velocities. Changes

in potential energy of the system implies changes in the kinetic energy so that its total energy remains constant. The dynamics of the collisions in **Paper III** were investigated in a *NVE* ensemble.

The constraint on the number of particles, volume and temperature defines the *NVT* ensemble. In this ensemble, the energies of the microstates can fluctuate while the system is kept in contact with the heat bath at temperature T. Possible ways for temperature control in an *NVT* ensemble are the use of inert carrier gas atoms or coupling the system to an artificial thermostat. The use of carrier gas is not computationally beneficial since it increases the number of interacting atoms. In this work the *Nosé-Hoover thermostat* (Martyna et al., 1992; Tobias et al., 1993) was used. We used the *NVT* ensemble exclusively to determine the initial positions and velocities of the clusters used in the dynamic simulations.

4 Using computational techniques to study SO₂ ionic oxidation products

Chemical reactions occur when nuclear configurations rearrange from the reactants state to the products state. In the case of polyatomic molecules, many possible rearrangement paths can connect the reactants to the products and different intermediates can also form along a given path as indicated in reaction (R1)

$$A + B \underset{k_{evap}}{\overset{k_{coll}}{\rightleftarrows}} AB \xrightarrow{k_{reac}} AB^{\ddagger} \longrightarrow \text{Products}, \tag{R1}$$
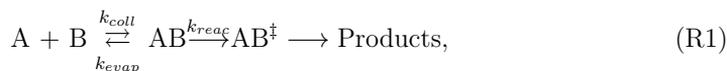
where k_{coll} is the collision rate constant of A and B, k_{evap} and k_{reac} are the evaporation rate constant and the reaction rate constant of the reactant complex AB, respectively. The question one can now ask is, how do these molecules interact? What properties of the reacting species are underlined? Computational methods provide valuable insights into understanding the mechanisms of chemical reactions. For example, quan-
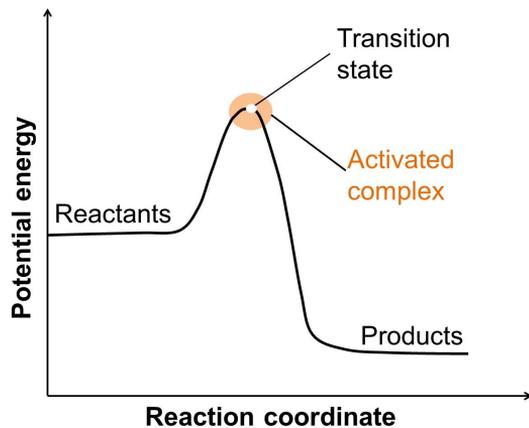

Figure 1: A reaction profile. The activated complex is the region near the potential energy maximum, and the transition state corresponds to the maximum itself.

tum chemical methods are used to directly determine the Gibbs free energy change of a reaction as $\Delta G = \sum G(\text{products}) - \sum G(\text{reactants})$, where G of a molecule or cluster is calculated with equation (28) or (29). The magnitude of ΔG determines the feasibility of a reaction: when ΔG is negative, then the reaction is thermodynamically

favourable at the conditions at which it is calculated. In some cases (such as in **Papers I & II**), the reaction proceeds through the formation of an activated complex ($AB^{\ddagger}$ in reaction R1 above) and a transition state as depicted in Figure 1 (Atkins and de Paula, 2006). If the activated complex passes through the transition state, then it forms the products of the reaction in the path considered. In other words, the reactants form new products by overcoming an energy barrier corresponding to the energy of the transition state and in this case, it is important to determine how fast the reactions take place, *i.e.,* to determine the reaction rate constants. The reactions investigated in this thesis are bimolecular. To determine the rate constants of such reactions, we built a kinetic model that takes into account the collision rate of the reactants, the reaction rate and the evaporation rate of the reactant complex. For a chosen path, we assume for simplicity no other sink of the reactant complex than its evaporation and its reaction to form the desired product. We also assume no other source of the reactant complex than from collision of A and B, and finally that the activation complex once formed, always react forwards to form the products. The kinetics of the reaction are determined by assuming *pseudo-steady state approximation* on the reactant complex,

$$k_{\text{coll}}[A][B] = (k_{\text{evap}} + k_{\text{reac}})\,[AB]. \tag{31}$$

The collision rate constant is generally determined from classical kinetic gas theory but for ion-dipole collisions, several parameterizations have been presented in the literature. The version by Su and Chesnavich (1982) was used in this thesis. The evaporation rate constant of the reactant complex was determined from the detailed balance condition (Vehkamäki, 2006; Ortega et al., 2012), while its reaction rate constant was determined from the transition state theory. In order to apply this theory, the configuration of the transition state and its energy have to be determined. In **Papers I** and **II**, the transition states were localized using quantum chemical methods, which proceed by gradually constraining the desired reaction coordinates of the reactant complex while optimizing the remainder of the configuration to form an activated complex. The configuration of the activated complex is refined thereafter using the *synchronous transit quasi-Newton* method (Peng et al., 1996) to form the transition state. A "*good*" transition state configuration should connect to the desired products of the reaction: this was ensured by performing the *intrinsic reaction coordinate* calculations (Fukui, 1981). The overall rate of reaction (R1), r_{R1}, is determined by the rate at which the reactant complex is converted into the product,

$$r_{\text{R1}} = k_{\text{reac}}[AB] = k_{\text{coll}}\frac{k_{\text{reac}}}{k_{\text{reac}} + k_{\text{evap}}}[A][B] = k_{\text{bimol}}[A][B], \tag{32}$$

where the bimolecular rate constant of the A + B reaction, k_{bimol}, is obtained by taking the expression of [AB] from equation (31). We applied this model to determine the rates of the $SO_2 + O_2^-$ and $SO_2 + SO_4^-$ reactions in **Papers I** and **II**, respectively.

4.1   From dynamics to reaction rate constants

First principles Molecular dynamics simulations are an effective approach to circumvent constraining the coordinates of the reactant complex in order to determine the transition state. This method has the advantage of allowing the system to propagate in time and therefore explores all intermediate steps of the reaction from separate reactants to the formation of the products. We used this method in **Paper III** to investigate the outcome of $O_3-SO_3SO_3^-(H_2O)_{0\text{-}2}$ collisions. The FPMD simulations technique assesses all likely reaction paths by sampling various collisions. Moreover, this method allows a
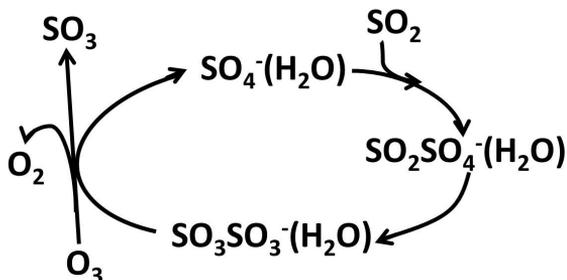

Figure 2: Schematic of the SO_4^--catalyzed SO_2 oxidation to SO_3 by O_3. A water molecule is more likely to attach to $SO_3SO_3^-$ (see **Paper II**).

direct evaluation of the steric, dynamic, and water effects on the collisions. Contrarily to the approach that combines quantum chemical methods with the transition state theory to determine reaction rates in terms of thermodynamic parameters, molecular dynamics simulations determine the reaction rates purely as the fraction of reactive collisions relative to the total collision rate. It means that if the collision rate constant is determined accurately, this approach provides best estimates for the reaction rate constants (Bork et al., 2013b). With this approach, the reaction rate for a given path

is given as

$$\text{reaction rate} = \frac{\text{number of reactive collisions}}{\text{total number of collisions}} \times \text{collision rate}, \qquad (33)$$

where the number of reactive collisions is the number of collisions leading to a particular reaction. The use of both quantum chemical and FPMD methods to investigate the reactions of **Papers II** and **III** led us to the path of Figure 2 where SO_4^- acts as a catalyst in the SO_2 oxidation to SO_3 by O_3. This mechanism constitutes a complementary source of atmospheric sulfuric acid, the key species in atmospheric particle formation.

4.2 Effects of hydration on reaction rate constants and electrical mobilities

Water is one of the most abundant trace gases in the troposphere, and is likely to bind to various clusters at ambient conditions. Although water does not bind as strongly as ammonia and amines to some clusters such as sulfuric acid-based clusters (Loukonen et al., 2010; Kurtén et al., 2007), it is known to affect the dynamics and the kinetics of reactions, as well as the growth of clusters (Bork et al., 2013a; Paasonen et al., 2012). We examined the effects of hydration on the reactions investigated in **Papers I, II** and **III**. Figure 3 shows the water effect on the reaction between SO_2 and SO_4^-. It is seen that the presence of water inhibits the formation of all intermediates in the reaction since less negative values of the Gibbs free energy are obtained when water is attached. It is also shown in **Paper II** that the rate of the reaction decreases with increasing hydration. For all the computational method used, the rate constants are calculated for reactions with and without water, wherefrom the overall reaction rate constant, k_{aver}, is calculated when weigthed by the likelihood of clustering with 0, 1, $\cdots$ N water molecules as

$$k_{\text{aver}} = \sum_{i=0}^{N} k_i \times x_i, \qquad (34)$$

where k_i is the rate constant of the reaction with i water molecules, and x_i is the relative concentration of the cluster containing i water molecules. N is the maximum number of water molecules that can be bound to the cluster. The relative concentration, x_i, of a hydrate containing i water molecules is calculated from the Gibbs free energy of the ith hydration, ΔG_i, using the law of mass action and by assuming thermal equilibrium
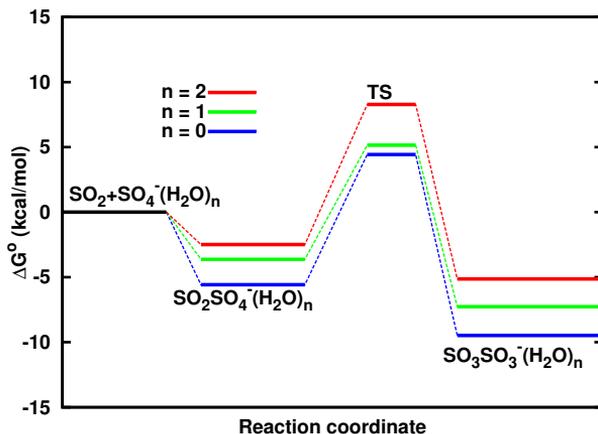
Figure 3: Energy surface of the $SO_2 + SO_4^-$ reaction at 1 atm and 298 K. All the energies are calculated relative to the $SO_2 + SO_4^-$ energy. "TS" denotes the transition state, and ΔG° is the Gibbs free energy change.

as (Noppel et al., 2002)

$$x_i = \frac{\left(\frac{P_{\text{water}}}{P_{\text{ref}}}\right)^i \exp\left(-\frac{\Delta G_i}{k_B T}\right)}{\sum_{i=0}^{N} \left(\frac{P_{\text{water}}}{P_{\text{ref}}}\right)^i \exp\left(-\frac{\Delta G_j}{k_B T}\right)}, \tag{35}$$

where P_{ref} is the pressure at which the Gibbs free energies are calculated, $P_{\text{water}} = \text{RH}/100 \times P_{\text{water}}^{\text{eq}}$ is the partial pressure of water vapor. RH is the relative humidity, and $P_{\text{water}}^{\text{eq}}$ is the equilibrium vapor pressure of water. Different parameterizations for the equilibrium vapor pressure of water exist but the version by Wagner and Pruss (1993), revised by Murphy and Koop (2005) was used.

Both ammonia and dimethylamine are known to stabilize sulfuric acid clusters and to enhance the formation rate of particles made of these clusters (Kirkby et al., 2011; Almeida et al., 2013). Water is often omitted in experimental studies of these clusters due to fast evaporation in the instrument. It was shown, however, using computational methods that depending on the degree of hydration the water content of electrically neutral clusters containing sulfuric acid, ammonia or dimethylamine is important (Henschel et al., 2014) and therefore water need to be included in simulations of sulfuric acid-based particle formation in order to mimic realistic situations. Electrically neutral clusters are in general more difficult to measure than charged ones. Electrically

neutral particles can be detected using Condensation Particle Counter techniques after enlarging them by condensing vapour like water or butanol (Lehtipalo, 2011), while charged particles can be detected directly with ion mobility spectrometers and mass spectrometers (Mirme et al., 2007; Tammet, 2006). Charged clusters or particles have the ability to move in response to the application of an electric field (de la Mora et al., 1998; Ehn et al., 2011): this property is called electrical mobility and is important in size-selected measurements invoving ion mobility spectrometers. Starting from their coordinates, the electrical mobilities of clusters containing one bisulfate ion, up to three sulfuric acids, ammonia or dimethylamine (known to form in the first steps of atmospheric particle formation) were calculated using a particle dynamics model (Larriba and Hogan, 2013a,b). The model is flexible enough to take in both dry and hydrated clusters. Amongst the inputs in this model are the clusters coordinates, the pressure, the temperature and the carrier gas, and the outputs are molecular cross sections and the electrical mobilities of clusters. The electrical mobility of a cluster was determined by weighting the electrical mobilities of its different hydrates by their relative concentrations to predict the effect of humidity. We found no profound effect of humidity on electrical mobilities of the investigated clusters, and we conclude that the mobilities of clusters formed in the first steps on atmospheric particle formation are weakly sensitive to humidity (**Paper IV**).

5 Review of papers and the author's contribution

The research presented in this thesis aims to provide mechanisms of reactions of SO_2 with some atmospheric ions, while examining the effect of hydration on the stability of the clusters and on the reaction rates. The effect of hydration is further extended to the stability and electrical mobilities of clusters containing one bisulfate, up to three sulfuric acids, ammonia or dimethylamine. A variety of computational methods are used.

Paper I studies the reaction between SO_2 and O_2^- at atmospheric conditions using quantum chemical calculations. This paper solves the discrepancy concerning the outcome of the $SO_2 + O_2^-$ reaction by providing its most likely mechanism. Regardless of hydration, the direct product of the SO_2 and O_2^- collision ($O_2SO_2^-$) is prevented from isomerising to the sulfate radical ion (SO_4^-) due to a very high energy barrier. The main product of this reaction is the peroxy form of SO_4^-. The author performed the calculations, analyzed the data and wrote most of the paper.

Paper II investigates the reaction between the sulfate radical ion and sulfur dioxide in the gas phase, using quantum chemical calculations. We calculate the formation free energies at 298 K and 1 atm of all intermediates in this reaction and examine the effect of hydration both on the binding strength of the clusters and on the reaction rate constants. We find that SO_4^- is a good SO_2 oxidant, especially at low relative humidity and high SO_2 concentration. The main product of the reaction is $SO_3SO_3^-$, found to be stable toward decomposition into the initial products. The author is responsible of performing all the calculations, analyzing the data and writing most of the paper.

Paper III presents a closure study of the reaction between SO_4^- and SO_2 investigated in **Paper II**, using First Principles Molecular Dynamics simulations. From a series of collisions between O_3 and $SO_3SO_3^-$, the hydration, orientation at impact, steric and dynamic effects on different pathways and outcomes are determined. The reaction rates are calculated as the ratio between reactive collisons of different paths and the total number of collisions. The majority of reactive collisions lead to the formation of SO_4^-, SO_3, and O_2. The rate of this reaction is estimated to be 30 % of the total collision rate, and it is concluded that SO_4^- is an efficient catalyst in SO_2 oxidation to SO_3 by O_3. The author is responsible of running all the simulations, analyzing all the data, and writing the paper.

Paper IV compares the binding strength of water on clusters containing one bisulfate ion, up to three sulfuric acids, and either ammonia or dimethylamine. We determine the Gibbs free energy of formation of different clusters as well as the Gibbs free energies of hydration using quantum chemical calculations. The Gibbs free energies of hydration are used in the law of mass action to determine the equilibrium hydrate distributions of the clusters at 298 K and relative humidities between 0 and 100 %. The calculated Gibbs free energies of hydration indicate that the binding of water is stronger to ammonia-containing clusters than to dimethylamine-containing and base-free clusters, which results in a wider hydrate distribution for ammonia-containing clusters. We further extend the effect of hydration on electrical mobilities calculated with a particle dynamics model. The results show that the effect of humidity is negligible on the electrical mobilities of clusters investigated. The author is responsible of performing all the calculations, analyzing the data and writing the paper.

6 Conclusions

The research presented in this thesis uncovers the most likely mechanisms of reactions of sulfur dioxide with the superoxide and the sulfate radical ions. By using a variety of computational methods including electronic structure calculations and first principles molecuar dynamics simulations, this research not only provides insights into the understanding of the atmospheric sulfur cycle, but it also complements various experimental studies on ion-induced SO_2 reactions (Möhler et al., 1992; Fahey et al., 1982; Fehsenfeld and Ferguson, 1974). The work of this thesis also examines the effect of hydration on the stability and electrical mobilities of clusters containing one bisulfate ion, up to three sulfuric acids, ammonia or dimethylamine.

The most stable structures and the Gibbs free energies of all intermediates in the $SO_2 + O_2^-$ reaction were determined in order to provide the most likely mechanism of the reaction at ambient conditions. Many experimenal studies based on mass spectrometry investigated the above mentioned reaction but discrepancies concerning the chemical structure of the final product prevailed. The expected structures of the product were assigned based on its further reactivity. Our calculations indicate that the immediate product of SO_2 and O_2^- collision, $SO_2O_2^-$, is unable to isomerize to the sulfate radical ion (SO_4^-) due to a very high energy barrier separating the two states. At 298 K and humidity below 50 %, the main product is $SO_2O_2^-$, structurally different from the sulfate radical ion. These results therefore solve the discrepancies arisen from experiments (Fahey et al., 1982; Shuie et al., 1993; Möhler et al., 1992; Vacher et al., 1992) concerning the structure of the $SO_2 + O_2^-$ reaction product.

The chemistry of SO_4^- was explored by reaction with SO_2 in the gas phase. The two species were experimentally found to cluster effectively but without further information on the structure of the final product (Fehsenfeld and Ferguson, 1974). Using quantum chemical calculations and the transition state theory, we determine the thermodynamics and the kinetics of the reaction at 298 K. It is found that at low relative humidity, SO_4^- reacts with SO_2 to form the $SO_3SO_3^-$ ion. Although the reaction is fast and energetically favourable, no further chemistry of $SO_3SO_3^-$ was established from earlier studies. Its decomposition by reaction with O_3 is further examined using first-principles molecular dynamics simulations. This method includes steric and dynamic effects in the collisions and scan all possible reaction paths. It is found that the majority of reactive

collisions lead to the formation of SO_4^-, SO_3, and O_2. This reaction proceeds at about 30 % of the total collision rate of $SO_3SO_3^-$ and O_3. Taking into account the formation of $SO_3SO_3^-$ from $SO_4^- + SO_2$ reaction, we conclude that SO_4^- acts as a catalyst in SO_2 oxidation by O_3 to SO_3. These results show that first principles methods are a viable tool to investigate reaction mechanisms and complement experimental observations.

The effect of hydration on electrical mobilities of clusters containing one bisulfate ion, up to three sulfuric acid and base (either ammonia or dimethylamine) molecules labelled as $[(HSO_4^-)(H_2SO_4)_{0-3}(\text{base})_{0-2}]$, was examined. The structures of each cluster were optimized using density functional theory and the coordinates of their most stable structures were used in a particle dynamics model (Larriba and Hogan, 2013a,b) to calculate their electrical mobilities in air. By weighting the electrical mobilities of the hydrates of different clusters by their respective relative concentration, we find no profound effect of humidity on the electrical mobilities of clusters formed in the first steps of atmospheric particle formation, as suggested by Jen et al. (2015). Our results further indicate that the effect of humidity on electrical mobilities is important only for clusters or ions with molecular weight below 100 Da.

References

Almeida, J., Schobesberger, S., Kürten, A., Ortega, I.K., Kupiainen-Määttä, O., Pra-plan, A.P., Adamov, A., Amorim, A., Bianchi, F., Breitenlechner, M., David, A., Dommen, J., Donahue, N.M., Downard, A., Dunne, E., Duplissy, J., Ehrhart, S., Flagan, R.C., Franchin, A., Guida, R., Hakala, J., Hansel, A., Heinritzi, M., Henschel, H., Jokinen, T., Junninen, H., Kajos, M., Kangasluoma, J., Keskinen, H., Kupc, A., Kurtén, T., Kvashin, A. N., Laak-sonen, A., Lehtipalo, K., Leiminger, M., Leppä, J., Loukonen, V., Makhmutov, V., Mathot, S., McGrath, M.J., Nieminen, T., Olenius, T., Onnela, A., Petäjä, T., Riccobono, F., Riipinen, I., Rissanen, M., Rondo, L., Ruuskanen, T., Santos, F.D., Sarnela, N., Schallhart, S., Schnitzhofer, R., Seinfeld, J.H., Simon, M., Sipilä, M., Stozhkov, Y., Stratmann, F., Tomé, A., Tröstl, J., Tsagkogeorgas, G., Vaattovaara, P., Viisanen, Y., Virtanen, A., Vrtala, A., Wagner, P.E., Weingartner, E., Wex, H., Williamson, C., Wimmer, D., Ye, P., Yli-Juuti, T., Carslaw, K.S., Kulmala, M., Curtius, J., Baltensperger, U., Worsnop, D.R., Vehkamäki, H., and Kirkby, J. (2013). Molecular understanding of sulphuric acid–amine particle nucleation in the atmosphere. *Nature*, 501:359–363.

Atkins, P. and de Paula, J. (2006). Physical Chemistry, 8th ed. Oxford University Press, New York.

Barone, V. (2004). Vibrational zero-point energies and thermodynamic functions beyond the harmonic approximation. *J. Chem. Phys.*, 120:3059–3065.

Becke, A.D. (1993). Density functional thermochemistry. III. The role of exact exchange. *J. Chem. Phys.*, 98: 5648–5652.

Berndt, T., Böge, O., and Stratmann, F. (2003). Gas-phase ozonolysis of a-pinene: gaseous products and particle formation. *Atmos. Environ.*, 37:3933–3945.

Berndt, T., Böge, O., and Stratmann, F. (2004). Atmospheric particle formation from the ozonolysis of alkenes in the presence of SO_2. *Atmos. Environ.*, 38:2145–2153.

Berndt, T, Stratmann, F., Bräsel, S., Heintzenberg, J., Laaksonen, A, and Kulmala, M. (2008). SO_2 oxidation products other than H_2SO_4 as a trigger of new particle formation. Part 1: Laboratory investigations. *Atmos. Chem. Phys.*, 8:6365–6374.

Bork, N., Kurtén, T., and Vehkamäki, H. (2013a). Exploring the atmospheric chemistry of $O_2SO_3^-$ and assessing the maximum turnover number of ion-catalysed H_2SO_4 formation. *Atmos. Chem. Phys.*, 13:3695–3703.

Bork, N., Loukonen, V., and Vehkamäki, H. (2013b). Reactions and reaction rate of atmospheric SO_2 and $O_3^-(H_2O)_n$ collisions via molecular dynamics simulations. *J. Phys. Chem. A*, 117:3143–3148.

Bork, N., Elm, J., Olenius, T., and Vehkamäki, H. (2014). Methane sulfonic acid-enhanced formation of molecularclusters of sulfuric acid and dimethyl amine. *Atmos. Chem. Phys.*, 14:12023–12030.

Boys, S.F. (1950). Electronic wave functions. I. A general method of calculations for the stationary states of any molecular system. *Proc. R. Soc. (London) A*, 200:542-554.

Ceperley, D.M., and Alder, B.J. (1980). Ground state of the electron gas by a stochastic method. *Phys. Rev. Lett.*, 45: 566–569.

Chaban, G.M., Jung, J.O., and Gerber, R.B. (1999). Ab initio calculation of anharmonic vibrational states of polyatomic systems: Electronic structure combined with vibrational self-consistent field. *J. Chem. Phys.*, 111:1823–1829.

Chen, H., Ezell, M. J., Arquero, K. D., Varner, M. E., Dawson, M. L., Gerber, R. B., and Finlayson-Pitts, B. J. (2015). New particle formation and growth from methane-sulfonic acid, trimethylamine and water. *Phys. Chem. Chem. Phys.*, 17:13699–13709.

Christiansen, O., Koch, H., and Jørgensen, P. (1995). The second-order approximate coupled cluster singles and doubles model CC2. *Chem. Phys. Lett.*, 243: 409–418.

de la Mora, J.F., de Luan, L., Thilo, E., Rosell, J. (1998). Differential mobility analysis of molecular ions and nanometer particles. *TrAC, Trends Anal. Chem.*, 17:328–339.

Dunning, T.H. (1989). Gaussian basis sets for use in correlated molecular calculations. I. The atoms boron through neon and hydrogen. *J. Chem. Phys.*, 90:1007–1023.

Ehn, M., Junninen, H., Petäjä, T., Kurtén, T., Kerminen, V.-M., Schobesberger, S., Manninen, H. E., Ortega, I. K., Vehkamäki, H., Kulmala, M., and Worsnop, D. R. (2010). Composition and temporal behavior of ambient ions in the boreal forest. *Atmos. Chem. Phys.*, 10:8513–8530.

Ehn, M., Juninen, H., Schobesberger, S., Manninen, H., Franchin, A., Sipilä , M., Petäjä, T., Kerminen, V.-M., Tammet, H., Mirme, A., Mirme, S., Hõrrak, U., Kulmala, M. and Worsnop, D.R. (2011). An instrumental comparison of mobility and mass measurements of atmospheric small ions. *Aerosol Sci. Technol.*, 45:522–532.

Ehn, M., Thornton, J.A., Kleist, E., Sipilä, M., Junninen, H., Pullinen, I., Springer, M., Rubach, F., Tillmann, R., Lee, B., Lopez-Hilfiker, F., Andres, St., Acir, I.-H., Rissanen, M., Jokinen, T., Schobesberger, S., Kangasluoma, J., Kontkanen, J., Nieminen, T., Kurtén, T., Nielsen, L. B., Jørgensen, S., Kjaergaard, H. G., Canagaratna, M., Dal Maso, M., Berndt, T., Petäjä, T., Wahner, A., Kerminen, V.-M., Kulmala, M., Worsnop, D. R., Wildt, J., and Mentel, T. F. (2014). A large source of low-volatility secondary organic aerosol. *Nature*, 506:476–479.

Enghoff, M. B., Bork, N., Hattori, S., Meusinger, C., Nakagawa, M., Pedersen, J. O. P., Danielache, S., Ueno, Y., Johnson, M. S., Yoshida, N., and Svensmark, H. (2012). An isotopic analysis of ionising radiation as a source of sulphuric acid. *Atmos. Chem. Phys.*, 12:5319–5327.

Fahey, D. W., Böhringer, H., Fehsenfeld, F. C., and Ferguson, E. E. (1982). Reaction rate constants for $O_2^-(H_2O)_n$ ions $n = 0$ to 4, with O_3, NO, SO_2, and CO_2. *J. Chem. Phys.*, 76:1799–1805.

Fehsenfeld, F. C. and Ferguson, E. E. (1974). Laboratory studies of negative ion reactions with atmospheric trace constituents. *J. Chem. Phys.*, 61:3181–3193.

Fukui, K. (1981). The path of chemical reactions – the IRC approach. *Accounts Chem. Res.*, 14:363–368.

Grimme, S., Antony, J., Ehrlich, S., and Krieg, H. (2010). A consistent and accurate ab initio parametrization of density functional dispersion correction (DFT-D) for the 94 elements H-Pu. *J. Chem. Phys.*, 132: 154104-1–154104-19.

Harris, E., Sinha, B., van Pinxteren, D., Tilgner, A., Fomba, K. W., Schneider, J., Roth, A., Gnauk, T., Fahlbusch, B., Mertes, S., Lee, T., Collett, J., Foley, S., Borrmann, S., Hoppe, P., and Herrmann, H. (2013). Enhanced role of transition metal ion catalysis during in-cloud oxidation of SO_2. *Science*, 340:727–730.

Hegg, D.A., Majeed, R., Yuen, P.F., Baker, M.B., and Larson, T.V. (1996). The impacts of SO_2 oxidation in cloud drops and in haze particles on aerosol light scattering and CCN activity. *Geophys. Res. Lett.* , 28: 2613–2616.

Henschel, H., Navarro, J. C. A., Yli-Juuti, T., Kupiainen-Määttä, O., Olenius, T., Ortega, I. K., Clegg, S. L., Kurtén, T., Riipinen, I., and Vehkamäki, H. (2014). Hydration of atmospherically relevant molecular clusters: computational chemistry and classical thermodynamics. *J. Phys. Chem. A*, 118: 2599–2611.

Hinds, W.C (1999). Aerosol Technology: Properties, Behavior, and Measurement of Airborne Particles. 2nd edition John Wiley & Sons, Inc., New York, NY, USA.

Ho, J. Coote, M.L., Cramer, C.J., and Truhlar, D.G. (2015). Theoretical calculation of reduction potentials" in organic electrochemistry. 5th Ed. O. Hammerich, B. Speiser, Eds. CRC Press: Boca Raton, FL.

Hohenberg, P., and Kohn, W. (1964). Inhomogeneous Electron Gas. *Phys. Rev.*, 136: B864–B871.

Hättig, C., and Weigend, F. (2000). CC2 excitation energy calculations on large molecules using the resolution of the identity approximation. *J. Chem. Phys.*, 113: 5154–5161.

IPCC (the Intergovernmental Panel on Climate Change) (2013). Climate Change 2013: The Physical Science Basis. Contribution of working group I to the fifth assessment report of the Intergovernmental Panel on Climate Change. Available online at https://www.ipcc.ch/pdf/assessment-report/ar5/wg1/WG1AR5_Frontmatter_FINAL.pdf. IPCC secretariat, Geneva, Switzerland.

Jen, C.N., Hanson, D.R., and McMurry, P.H. (2015). Toward reconciling measurements of atmospherically relevant clusters by chemical ionization mass spectrometry and mobility classification/vapor condensation. *Aerosol Sci. Tech.*, 49:i–iii.

Jensen, F. (2007). Introduction to Computational Chemistry. John Wiley & Sons Ltd., West Sussex, U.K.

Junninen, H., Ehn, M., Petäjä, T., Luosujärvi, L., Kotiaho, T., Kostiainen, R., Rohner, U., Gonin, M., Fuhrer, K., Kulmala, M., and Worsnop, D. R. (2010). A high-resolution mass spectrometer to measure atmospheric ion composition. *Atmos. Meas. Tech.*, 3:1039–1053.

Kathmann, S., Schenter, G., and Garrett, B. (2007). The Critical Role of Anharmonicity in Aqueous Ionic Clusters Relevant to Nucleation. *J. Phys. Chem. C*, 111:4977–4983.

Kirkby, J., Curtius, J., Almeida, J., Dunne, E., Duplissy, J., Ehrhart, S., Franchin, A., Gagné, S., Ickes, L., Kürten, A., Kupc, A., Metzger, A., Riccobono, F., Rondo, L., Schobesberger, S., Tsagkogeorgas, G., Wimmer, D., Amorim, A. Bianchi, F.,

Breitenlechner, M., David, A., Dommen, J., Downard, A., Ehn, M., Flagan, R. C., Haider, S., Hansel, A., Hauser, D., Jud, W., Junninen, H., Kreissl, F., Kvashin, A., Laaksonen, A., Lehtipalo, K., Lima, J., Lovejoy, E. R., Makhmutov, V., Mathot, S., Mikkilä, J., Minginette, P., Mogo, S., Nieminen, T., Onnela, A., Pereira, P., Petäjä, T., Schnitzhofer, R., Seinfeld, J. H., Sipilä, M., Stozhkov, Y., Stratmann, F., Tomé, A., Vanhanen, J., Viisanen, Y., Vrtala, A., Wagner, P. E., Walther, H., Weingartner, E., Wex, H., Winkler, P. M., Carslaw, K. S., Worsnop, D. R., Baltensperger, U., and Kulmala, M. (2011). Role of sulphuric acid, ammonia and galactic cosmic rays in atmospheric aerosol nucleation. *Nature*, 476:429–433.

Kohn, W., and Sham, L.J. (1964). Self-condistent equations including exchange and correlation effects. *Phys. Rev.*, 140: A1133–A1138.

Kuang, C., McMurry, P.H., McCormick, A.V., and Eisele, F.L. (2008). Dependence of nucleation rates on sulfuric acid vapor concentration in diverse atmospheric locations. *J. Geophys. Res.*, 113:D10209.

Kurtén, T., Torpo, L., Ding, C.-G., Vehkamäki, H., Sundberg, M.R., Laasonen, K., and Kulmala, M. (2007). A density functional study on water-sulfuric acid-ammonia clusters and implications for atmospheric cluster formation. *J. Geophys. Res.*, 12:D04210.

Kurtén, T., Loukonen, V., Vehkamäki, H., and Kulmala, M. (2008). Amines are likely to enhance neutral and ion-induced sulfuric acid-water nucleation in the atmosphere more effectively than ammonia. *Atmos. Chem. Phys.*, 8:4095–4103.

Laaksonen, A, Kulmala, M, Berndt, T, Stratmann, F., Mikkonen, S., Ruuskanen, A., Lehtinen, K. E. J., Dal Maso, M., Aalto, P., Petäjä, T., Riipinen, I., Sihto, S.-L., Janson., R., Arnold, F., Hanke, M., Ücker, J., Umann, B., Sellegri, K., O'Dowd, C. D., and Viisanen, Y. (2008). SO_2 oxidation products other than H_2SO_4 as a trigger of new particle formation. Part 2: Comparison of ambient and laboratory measurements, and atmospheric implications. *Atmos. Chem. Phys.*, 8:7255–7264.

Larriba, C. and Hogan, C.J. (2013a). Ion mobilities in diatomic gases: measurement versus prediction with non-specular scattering models. *J. Phys. Chem. A*, 117:3887–3901.

Larriba, C. and Hogan, C.J. (2013b). Free molecular collision cross section calculation methods for nanoparticles and complex ions with energy accommodation. *J. Compu. Phys.*, 251:344–363.

Lehtipalo, K. (2011). How the development of condensation particle counters is reforming our view on atmospheric nucleation. Academic dissertation. Report Series in Aerosol Science, 123, University of Helsinki.

Loukonen, V., Kurtén, T., Ortega, I.K., Vehkamäki, H., Pádua, A.A.H., Sellegri, K., and Kulmala, M. (2010). Enhancing effect of dimethylamine in sulfuric acid nucleation in the presence of water – a computational study. *Atmos. Chem. Phys.*, 10:4961–4974.

Loukonen, V., Kuo, I-F. W., McGrath, M. J., and Vehkamäki, H. (2014). On the stability and dynamics of (sulfuric acid) (ammonia) and (sulfuric acid) (dimethylamine) clusters: A first-principles molecular dynamics investigation. *Chem. Phys.*, 428:164–174.

Martyna, G. J., Klein, M. L., and Tuckerman, M. E. (1992). Nosé-Hoover chains: The canonical ensemble via continuous dynamics. *J. Chem. Phys.*, 97:2635–2643.

Marx, D., and Hutter, J. (2009). Ab Initio Molecular Dynamics: Basic Theory and Advanced Methods. Cambridge University Press, Cambridge, UK.

Mauldin III, R. L., Berndt, T., Sipilä, M., Paasonen, P., Petäjä, T., Kim, S., Kurtén, T., Stratmann, F., Kerminen, V.-M., and Kulmala, M. (2012). A new atmospherically relevant oxidant of sulphur dioxide. *Nature*, 488:193–196.

McQuarrie, D. A. (1973). Statistical Thermodynamics. Harper & Row, Publishers,Inc., New York, NY., USA.

Mirme, A., Tamm, E., Mordas, G., Vana, M., Uin, J., Mirme, S., Bernotas, T., Laakso, L., Hirsikko, A., and Kulmala, M. (2007). A wide-range multi-channel air ion spectrometer. *Boreal Environ. Res.*, 12:247–264.

Murphy, D.M. and Koop, T. (2005). Review of the vapour pressures of ice and supercooled water for atmospheric applications. *Q. J. R. Meteorol. Soc.*, 131:1539–1565.

Moller, C. and Plesset, M. S. (1934). Note on an approximation treatment for many-electron systems. *Phys. Rev.*, 46: 618–622.

Möhler, O., Reiner, T., and Arnold, F. (1992). The formation of SO_5^- by gas phase ion-molecule reactions. *J. Chem. Phys.*, 97:8233–8239.

Nel, A. (2005). Air pollution-related illness: effects of particles. *Science*, 308:805–806.

Nieminen, T., Manninen, H.E., Sihto, S.-L., Yli-Juuti, T., Mauldin III, R.L., Petäjä, T., Riipinen, I., Kerminen, V.-M., and Kulmala, M. (2009). Connection of sulfuric acid to at-mospheric nucleation in boreal forest. *Environ. Sci. Technol.*, 43:4715–4721.

Noppel, M., Vehkamäki, H., and Kulmala, M. (2002). An improved model for hydrate formation in sulfuric acid–water nucleation. *J. Chem. Phys.*, 116:218–228.

Olenius, T., Schobesberger, S., Kupiainen-Määttä, O., Franchin, A., Junninen, H., Ortega, I. K., Kurtén, T., Loukonen, V., Worsnop, D. R., Kulmala, M., and Vehkamäki, H. (2013). Comparing simulated and experimental molecular cluster distributions. *Faraday Discuss.*, 165: 75–89.

Olsen, R., Kroes, G., Henkelman, G., Arnaldsson, A., and Jónsson, H. (2004). Comparison of methods for finding saddle points without knowledge of the final states. *J. Chem. Phys.* 121:9776–9792.

Omar, S.H. and Al-Wabel, N.A. (2010). Organosulfur compounds and possible mechanism of garlic in cancer. *Saudi Pharm. J.*, 18:51–58.

Ortega, I.K., Kupiainen, O., Kurtén, T., Olenius, T., Wilkman, O., McGrath, M.J., Loukonen, V., and Vehkamäki, H. (2012). From quantum chemical formation free energies to evaporation rates. *Atmos. Chem. Phys.*, 12:225–235.

Paasonen, P., Olenius, T., Kupiainen, O., Kurtén, T., Petäjä, T., Birmili, W., Hamed, A., Hu, M., Huey, L.G., Plass-Duelmer, C., Smith, J.N., Wiedensohler, A., Loukonen, V., McGrath, M.J., Ortega, I.K., Laaksonen, A., Vehkamäki, H., and Kulmala, M. (2012). On the formation of sulphuric acid − amine clusters in varying atmospheric conditions and its influence on atmospheric new particle formation. *Atmos. Chem. Phys.*, 12:9113–9133.

Parcell, S. (2002). Sulfur in human nutrition and applications in medicine. *Altern. Med. Rev.*, 7:22–44.

Peng, C., Ayala, P.Y., Schlegel, H.B., and Frisch, M.J. (1996). Using redundant internal coordinates to optimize equilibrium geometries and transition states. *J. Comput. Chem.*, 17:49–56.

Perdew, J.P., Chevary, J.A., Vosko, S.H., Jackson, K.A., Pederson, M.R. and Singh D.J. (1992). Atoms, molecules, solids, and surfaces: Applications of the generalized gradient approximation for exchange and correlation. *Phys. Rev. B*, 46: 6671-6687.

Perdew, J.P., Burke, K., and Ernzerhof, M. (1996b). Generalized gradient approximation for the exchange-correlation hole of a many-electron system *Phys. Rev. B*, 54: 16533–16539.

Perdew, J.P., Burke, K., and Ernzerhof, M. (1996b). Generalized gradient approximation made simple. *Phys. Rev. Lett.*, 77: 3865–3868.

Purvis, G. D. and Bartlett, R. J. (1982). A full coupled cluster singles and doubles model: the inclusion of disconnected triples. *J. Chem. Phys.*, 76: 1910–1918.

Ramanathan, V., Crutzen, P.J, Kiehl, J.T., and Rosenfeld, D. (2001). Aerosols, climate, and the hydrological cycle . *Science*, 294:2119–2124.

Riccobono, F., Schobesberger, S., Scott, C.E., Dommen, J., Ortega, I.K., Rondo, L., Almeida, J., Amorim, A., Bianchi, F., Breitenlechner, M., David, A., Downard, A., Dunne, E.M., Duplissy, J., Ehrhart, S., Flagan, R.C., Franchin, A., Hansel, A., Junninen, H., Kajos, M., Keskinen, H., Kupc, A., Kürten, A., Kvashin, A.N., Laaksonen, A., Lehtipalo, K., Makhmutov, V., Mathot, S., Nieminen, T., Onnela, A., Petäjä, T., Praplan, A.P., Santos, F.D., Schallhart, S., Seinfeld, J.H., Sipilä, M., Spracklen, D.V., Stozhkov, Y., Stratmann, F., Tomé, A., Tsagkogeorgas, G., Vaattovaara, P., Viisanen, Y., Vrtala, A., Wagner, P.E., Weingartner, E., Wex, H., Wimmer, D., Carslaw, K.S., Curtius, J., Donahue, N.M., Kirkby, J., Kulmala, M., Worsnop, D.R., and Baltensperger, U. (2014). Oxidation products of biogenic emissions contribute to nucleation of atmospheric particles. *Science*, 344:717–721.

Scott, A. P. and Radom, L. (1996). Harmonic vibrational frequencies: an evaluation of Hartree-Fock, Møller-Plesset, quadratic configuration interaction, density functional theory, and semiempirical scale factors. *J. Phys. Chem.*, 100:16502–16513.

Seinfeld, J.H., and Pandis, S.N. (2006). Atmospheric Chemistry and Physics: From Air Pollution to Climate Change. John Wiley & Sons, Inc., New York.

Shuie, L.-R., D'sa, E.D., Wentworth, W.E., and Chen, E.C.M. (1993). The determintion of thermodynamics of oxygen complexes of anions of sulfur dioxide and fluoronitrobenzens using atmospheric pressure ionization mass spectrometry. *Struct. Chem.*, 4:213–218.

Shukla, J.B., Sundar, S., Shivangi, and Naresh, R. (2013). Modeling and analysis of the acid rain formation due to precipitation and its effect on plant species. *Nat. Resour. Model.*, 26:53–65.

Slater, J.C. (1930). Atomic Shielding constants. *Phys. Rev.*, 36: 57–64.

Stieb, D.M., Judek, S., and Burnett, R.T. (2002). Meta-analysis of time-series studies of air pollution and mortality: effects of gases and particles and the influence of cause of death, age, and season. *J. Air. & Waste Manage. Assoc.*, 52:470–484.

Szabo, A., and Ostlund, N.S. (1996). Modern Quantum Chemistry. Introduction to Advanced Electronic Structure Theory. Dover Publications, Inc., Mineola, NY, USA. *Unabridged and unaltered republication of the "First Edition, Revised," originally published by the McGraw-Hill Publishing Company, New York, 1989. The original edition was published by the Macmillan Publishing Company, New York, 1982.*

Tammet, H. (2006). Continuous scanning of the mobility and size distribution of charged clusters and nanometer particles in atmospheric air and the Balanced Scanning Mobility Analyzer BSMA. *Atmos. Res.*, 82:523–535.

Tobias, D.J., Martyna, G.J., and Klein, M.L. (1993). Molecular Dynamics Simulations of a Protein in the Canonical Ensemble. *J. Phys. Chem.*, 97:12959–12966.

Su, T. and Chesnavich, W.J. (1982). Parametrization of the ion-polar molecule collision rate constant by trajectory calculations. *J. Chem. Phys.*, 76:5183–5185.

Vacher, J.R, Jorda, M., Le Due, E., and Fltalre, M. (1992). A determination of the stabilities of negative ion clusters in SO_2 and SO_2-O_2 mixtures. *Int. J. Mass Spectrom. Ion Processes*, 114:149–162.

VandeVondele, J., Krack, M., Mohamed, F., Parrinello, M. Chassaing, T. and Hutter, J. (2005). QUICKSTEP: fast and accurate density functional calculations using a mixed gaussian and plane waves approach. *Comput. Phys. Commun.*, 167:103–128.

Vehkamäki, H. (2006). Classical Nucleation Theory in Multicomponent Systems. Springer, Berlin.

Wagner, W., and Pruss, A. (1993). International equations for the saturation properties of ordinary water substance. Revised according to the international temperature scale of 1990. Addendum to J. Phys. Chem. Ref. Data 16, 893 (1987). *J. Phys. Chem. Ref. Data*, 22:783–787.

Welz, O., Savee, J. D., Osborn, D. L., Vasu, S. S., Percival, C. J., Shallcross, D. E., and Taatjes, C. A. (2012). Direct kinetic measurements of criegee intermediate (CH_2OO) formed by reaction of CH_2I with O_2. *Science*, 335:204–207.

Werner, H.-J., Knowles, P. J., Knizia, G., Manby, F. R., Schütz, M., Celani, P., Korona, T., Lindh, R., Mitrushenkov, A., Rauhut, G., Shamasundar, K. R., Adler, T. B., Amos, R. D., Bernhardsson, A., Berning, A., Cooper, D. L., Deegan, M. J. O., Dobbyn, A. J., Eckert, F., Goll, E., Hampel, C., Hesselmann, A., Hetzer, G., Hrenar, T., Jansen, G., Köppl, C., Liu, Y., Lloyd, A. W., Mata, R. A., May, A. J., McNicholas, S. J., Meyer, W., Mura, M. E., Nicklass, A., O'Neill, D. P., Palmieri, P., Peng, D., Pflger, K., Pitzer, R., Reiher, M., Shiozaki, T., Stoll, H., Stone, A. J., Tarroni, R., Thorsteinsson, T., and Wang, M. (2012). MOLPRO, version 2012.1, a package of ab initio programs. available at: `http://www.molpro.net`.

Yanai, T., Tew, D.P., and Handy, N.C. (2004). A new hybrid exchange-correlation functional using the Coulomb-attenuating method (CAM-B3LYP). *Chem. Phys. Lett.*, 393: 51–57.

Yu, S., Saxena, V.K., and Zhao, Z. (2001). A comparison of signals of regional aerosol-induced forcing in Eastern China and the Southeastern United States. *Geeophys. Res. Let.*, 28:713–716.